Eur Biophys J (1990) 18:193–201

European Biophysics Journal

Quantitative conformational analysis of cytochrome *c* bound to phospholipid vesicles studied by resonance Raman spectroscopy

P. Hildebrandt*, T. Heimburg, and D. Marsh**

Max-Planck-Institut für Biophysikalische Chemie, Abteilung Spektroskopie, D-3400 Göttingen, Federal Republic of Germany

Received November 3, 1989/Accepted January 2, 1990

Abstract. Resonance Raman spectra have been recorded from ferri-cytochrome *c* bound to phospholipid vesicles composed of dimyristoyl phosphatidylglycerol (DMPG), dioleoyl phosphatidylglycerol (DOPG) or dioleoyl phosphatidylglycerol–dioleoyl phosphatidylcholine (DOPG-DOPC) (70 : 30 mole/mole). Lipid binding induces very significant conformational changes in the protein molecule. The resonance Raman spectra differ in their content of bands originating from two different conformational species, I and II, of the protein, and from two different spin and coordination states of the heme in conformation II. Data of sufficiently high precision were obtained that the spectra of the individual species could be quantitated by a constraint interative fitting routine using single Lorentzian profiles. In the high frequency, or marker band region (1200 to 1700 cm^{-1}), the frequencies, half widths and relative intensities of the individual bands could be estimated from previous surface enhanced resonance Raman measurements on cytochrome *c* adsorbed on a silver electrode. These were then further optimized to yield both the spectral parameters and relative contents of the different species. In the low frequency, or fingerprint, region (200 to 800 cm^{-1}), the spectral parameters of the individual species were obtained from difference spectra derived by sequential subtraction between the spectra of ferri-cytochrome *c* in the three different lipid systems, using the relative proportions of the species derived from the marker band region. These parameters were then subsequently refined by iterative optimization. The optimized spectral parameters in both frequency regions for the six-coordinated low spin states I and II, and for the five-coordinated high spin state II are presented. The proportion of state II, in which hence the heme crevice assumes an open structure, and of the five-coordinated high spin configuration, is found to increase on binding ferri-cytochrome *c* to negatively charged lipid vesicles. The extent of this conformational change increases in the order: DOPG-DOPC < DOPG < DMPG, with a parallel decrease of the proportion of the conformational state I, whose structure is similar to that of the uncomplexed ferri-cytochrome *c* in solution. Similar conformational changes are found for ferro-cytochrome *c* compared to those obtained with the oxidized species on binding to lipids. The present work is essential for studies which seek to analyze, in any detailed fashion, the conformational transitions in the heme protein which take place in response to changes in the lipid environment.

Key words: Cytochrome *c* – Phospholipid vesicles – Resonance Raman spectroscopy

Introduction

In previous studies, the structure and electron transfer properties of the heme protein, cytochrome *c* (cyt *c*), bound to charged surfaces were investigated by both normal resonance Raman (RR) and surface enhanced RR (SERR) spectroscopy (Hildebrandt and Stockburger 1989a, b). These techniques selectively probe the vibrational structure of the heme chromophore, yielding information on the conformation of the heme and its interactions with the immediate protein environment (Cotton et al. 1980; Spiro 1983; Smulevich and Spiro 1985; de Groot and Hester 1987; Kitagawa and Ozaki 1987; Wolf et al. 1988; Niki et al. 1989; Verma et al. 1989). A detailed analysis was carried out for cyt *c* adsorbed at the silver electrode/electrolyte interface (Hildebrandt and Stockburger 1989a). Two stable conformational states (designated I and II) could be identified, that differ with respect to the coordination pattern of the heme iron and the structure of the heme pocket. In state I (cyt_I), the structure of the protein remains largely unchanged relative to the native cyt *c* in solution, while in state II (cyt_{II}) the axial met-Fe bond is weakened, leading to a thermal equilibri-

* *Present address and address for offprint requests:* Max-Planck-Institut für Strahlenchemie, Stiftstrasse 34–36, D-4330 Mülheim, Federal Republic of Germany

** *Present address:* Department of Biochemistry, University of Virginia, Charlottesville, VA 22908, USA

um between a six-coordinated low spin (6cLS) and a five-coordinated high spin (5cHS) configuration. These structural changes are induced by electrostatic interactions of the basic protein with the charged electrode surface. It has also been demonstrated that similar conformational transitions can occur at charged interfaces other than the electrode surface, if they provide the necessary negatively charged binding sites for the positively charged front surface of the cyt *c* molecule (Hildebrandt and Stockburger 1989b). Thus it was suggested that the formation of the conformational states I and II is a general property of cyt *c* under the influence of strong electrostatic fields and hence may affect the electron transfer reactions of cyt *c* with its physiological redox partners, cytochrome oxidase (cyt.ox) and cytochrome reductase (cyt.red).

In order to check these conclusions we have extended our RR investigations of cyt *c* at charged interfaces to include biologically relevant systems. We have chosen anionic phospholipid vesicles which have the advantage of being a more realistic model for biological interfaces. In addition, such a study may provide valuable information about the role of phospholipids in the mitochondrial electron transport process between the membrane bound redox enzyme complexes. Furthermore, the cyt *c*/lipid system is of particular interest within the wider context of membrane interactions with peripheral proteins. Taking cyt *c* as a representative extrinsic protein, this system has been frequently studied by physico-chemical techniques in order to understand the molecular function of charged lipids in the activation of peripherally bound enzymes, in general (for example Azzi et al. 1969; Kimelberg et al. 1970; Deveaux et al. 1986; Peschke and Möhwald 1987)

In preliminary RR experiments in this study it was found that the conformational changes of cyt *c*, which are induced in these complexes, depend on a variety of parameters, which control the structure of the phospholipid vesicles, such as the temperature and the lipid composition. Hence, it turned out that a prerequisite for elucidating the interdependence between the conformational changes of cyt *c* and the structural and electrostatic properties of the phospholipid vesicles is the quantitative analysis of the RR spectra of these systems.

Thus the principal goal of the present study is to develop methods for the quantitation of the spectral changes and to assign these to the various conformational states of the cyt *c* in different lipid environments. It was found possible to obtain consistent results from both the low frequency and high frequency regions of the RR spectrum, by comparing cyt *c* in three different lipid systems, which induce quite distinct conformational changes in the protein.

Experimental

Cytochrome *c* (horse heart, type VI, Sigma, St. Louis, MO) was purified according to Brautigan et al. (1978) and converted to the oxidized form (cyt^{3+}) by addition of an excess of $K_3Fe(CN)_6$. The protein was then dialyzed extensively against buffer (1 m*M* Hepes, 1 m*M* EDTA, pH 7.5), which was found to be necessary to prevent photo-induced oxidation of the cyt *c* by the exciting laser beam. Dimyristoyl phosphatidylglycerol (DMPG) and dioleoyl phosphatidylglycerol (DOPG) were obtained from Avanti Polar Lipids, Inc. (Pelham, Al). Dioleoyl phosphatidylcholine (DOPC) was obtained from Sigma, St. Louis, MO.

Lipid vesicles were prepared by suspending the vacuum dried lipids (mixed previously in CH_2Cl_2) in aqueous buffer (1 m*M* Hepes, 1 m*M* EDTA, pH 7.5). The complexes with cyt *c* were formed by adding the protein to the lipid suspension. The final concentration of cyt *c* was 20 μ*M* and the cyt *c*/lipid ratio was adjusted to ensure that more than 97% of the protein was bound. Such concentration ratios were calculated from the binding curves which were determined by Heimburg (1989). Samples containing unsaturated lipids were kept under nitrogen or argon during preparation and measurement. Reduction of the lipid-bound cyt^{3+} was achieved by addition of dithionite to the carefully deoxygenated sample. In order to avoid an excess of the reductant, reduction was monitored using the characteristic RR bands of the oxidized and reduced forms.

The RR spectra were excited using the 407 nm line of a Kr^+ laser. Details of the experimental set-up are described elsewhere (Hildebrandt and Stockburger 1989b). The sample was contained in a rotating cuvette in order to avoid heating by the exciting beam (40 mW at the sample). For room temperature measurements (20 °C), a divided cell was used that allowed quasi-simultaneous measurement of two different samples, yielding optimum conditions for difference spectroscopy (principles of this technique are described by Rousseau (1981)). For variable temperature measurements, the rotating cell was enclosed in a thermostated chamber suitable for temperature control between 5° and 40 °C with an accuracy of ±0.5 °C. All RR spectra were recorded with a slit width of 2.7 cm^{-1}. For band fitting, the spectra were recorded with a step width of 0.2 cm^{-1}, and a program similar to that described by Fraser and Suzuki (1970) and documented by Alshuth (1985) was used. The fitting routine is based on a least squares optimization and permits temporary fixation of the individual fitting parameters and modification of the weighting factors. This offers the advantage that variation of those parameters which are known a priori with some confidence can be limited in the fitting routine. The RR bands were simulated with Lorentzian lineshapes which were shown to be appropriate in the case of cyt *c*. The baseline was simulated by a linear curve.

Results and discussion

Spectral indicators for conformational changes in cytochrome c

Figure 1 A shows the RR spectrum of cyt^{3+} in buffered solution (cyt^{3+}/H_2O) in the range below 800 cm^{-1}. The spectrum displays a complex pattern of bands which originate from vibrations involving high contributions of the peripheral substituents of the heme (Spiro 1983; Choi and Spiro 1983; Lee et al. 1986; Kitagawa and Ozaki 1987).

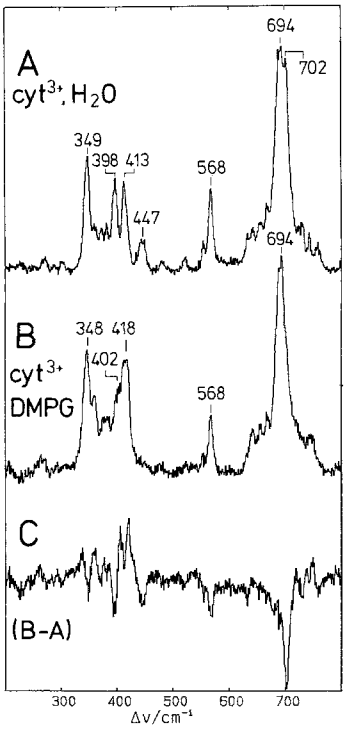

Fig. 1 A–C. Low frequency region of the RR spectra of cyt^{3+} excited at 407 nm. **A** in aqueous solution, and **B** bound to DMPG dispersion. **C** difference spectrum B–A. Spectra recorded at 20 °C

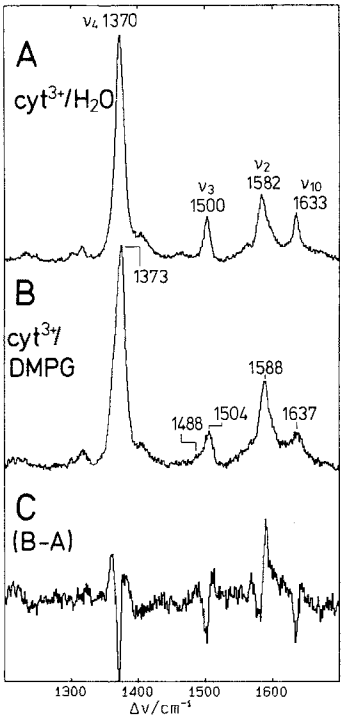

Fig. 2 A–C. High frequency region in the RR spectra of cyt^{3+} excited at 407 nm. **A** in aqueous solution, and **B** bound to DMPG dispersions. **C** difference spectrum: B–A. Spectra recorded at 20 °C

Therefore, these bands sensitively respond to steric and electrostatic interactions of the heme side chains with the protein matrix. In this way, this part of the spectrum, in particular the bands between 200 and 500 cm^{-1}, can be regarded as a fingerprint region for the specific structure of the heme pocket. For cyt^{3+}/H_2O, these bands have a unique pattern which clearly differs from that of other heme proteins or model compounds. The number of bands is almost doubled compared to, for example, hemoglobin (Choi and Spiro 1983). This pattern is therefore taken as a characteristic indicator of the closed heme crevice in cyt^{3+}/H_2O (Hildebrandt and Stockburger 1989a, b).

On the other hand, in the conformational state II of cyt^{3+} (cyt^{3+}_{II}), which is formed on adsorption at charged surfaces, the heme pocket is more open, as is reflected, for example, by the loss of the band at 446 cm^{-1} (Hildebrandt and Stockburger 1989a, b). In fact, the binding of cyt^{3+} to negatively charged lipid vesicles leads to a large decrease in intensity of this latter band (see Fig. 1 B). In addition to this band, the changes induced on binding cyt^{3+} to anionic lipid vesicles extend throughout the RR spectral range. They are particularly marked in the fingerprint region, and for the 694 cm^{-1} band, as is shown by the difference spectrum in Fig. 1 C. This difference spectrum was obtained by subtracting the spectrum in Fig. 1 B from that in Fig. 1 A, both of which were measured quasi-simultaneously in a divided cell.

Figure 2 gives the corresponding set of spectra for the high frequency range (1200 to 1700 cm^{-1}) which includes the oxidation- and spin-state marker bands ν_4, ν_3, ν_2, and ν_{10}. For these modes correlations between the frequencies and the electronic configuration and ligation state of the heme iron are well established (Spiro 1983; Parthasarathi et al. 1987; Kitagawa and Ozaki 1987). For cyt^{3+}/H_2O, these marker bands are located at 1370 (ν_4), 1500 (ν_3), 1582 (ν_2) and 1633 cm^{-1} (ν_{10}), which are expected positions for a ferric 6cLS heme (Fig. 2 A). In the RR spectrum of cyt^{3+} bound to negatively charged phospholipid vesicles, there is a broadening of these peaks which is accompanied by frequency shifts of up to 6 cm^{-1} (see Fig. 2 B). These spectral changes are more clearly seen in the difference spectrum (Fig. 2 C).

We now consider the spin state marker band ν_3 in more detail. Figure 3 gives the RR spectra of cyt^{3+} associated with three different anionic lipid systems, DMPG, DOPG, and DOPG-DOPC (70 : 30 Mole/Mole). It can be readily seen that both the location of the peak maxima and the shape of the spectra differ between these systems. For cyt^{3+}/DMPG (Fig. 3 A), there is a distinct shoulder at 1488 cm^{-1} accompanying the broad peak with maximum at 1504 cm^{-1}. For cyt^{3+}/DOPG (Fig. 3 B), this latter peak shifts down to 1502 cm^{-1} together with a decrease in intensity of the low frequency shoulder. Finally, in cyt^{3+}/DOPG-DOPC (Fig. 3 C), this peak sharpens and exhibits a maximum at 1500 cm^{-1}. Comparison of these profiles, show that there must be three bands which contribute in different degrees to the RR spectra of the three samples. These are located at ~1488, 1500, and 1504 cm^{-1}. While the 1488 cm^{-1} band lies in the range expected for a 5cHS configuration, the other bands must originate from 6cLS configurations (Parthasarathi et al. 1987). These estimated band locations are very similar to those found for the conformational states I and II of

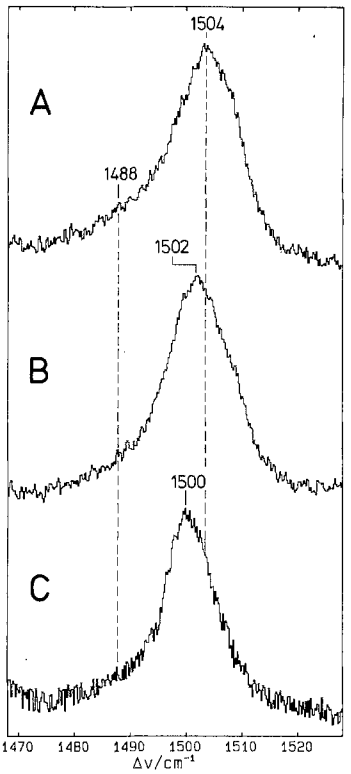

Fig. 3 A–C. RR spectra (ν_3 mode region) of cyt^{3+} bound to different anionic lipid dispersions. **A** DMPG recorded at 30 °C, **B** DOPG recorded at 20 °C, **C** DOPG-DOPC (70 : 30 mole/mole) recorded at 20 °C. Excitation at 407 nm

cyt^{3+} at the silver electrode, where the frequencies of the ν_3 mode were found to lie at 1499.5 cm^{-1} (cyt^{3+}_{I} 6cLS), 1503.1 cm^{-1} (cyt^{3+}_{II} 6cLS) and 1488.4 cm^{-1} (cyt^{3+}_{II} 5cHS) (Hildebrandt and Stockburger 1989a). This therefore indicates that these states also coexist in cyt^{3+} bound to negatively charged lipid vesicles.

Summarizing this overview of the entire RR spectrum of cyt^{3+} bound to phospholipid vesicles, we have two separate spectral regions (fingerprint and marker bands) which distinctly reflect the conformational and spin state changes on association of cyt^{3+} with lipid membranes. These regions therefore provide complementary information regarding the structure of the heme pocket and the coordination shell of the heme iron. Quantitative analysis of the two spectral regions is given below.

Quantitative analysis of the marker band region

The principal goal of the quantitative analysis is the evaluation of the relative RR intensities, I_{ij}, of the individual species, j, which are related to the relative concentrations, c_{ij}, by:

$$c_{ij} = f_{ij} \cdot I_{ij} \tag{1}$$

where f_{ij} are constants which are proportional to the Raman cross section of the mode *i*. The marker bands corresponding to the modes ν_4 and ν_3 were selected, since these have a high intensity and are well separated from other vibrational modes (see Fig. 4A). From the discussion in the preceeding section, it is clear that three bands must be considered for each mode, corresponding to three different species. Each of the modes is defined by I_{ij}, the frequency, ν_{ij}, and the half width $\Delta\nu_{ij}$. Unfortunately, the measured RR profiles in the ν_3 band region and, in particular in the ν_4 band region, are not well structured. Thus simulation based on nine freely adjustable parameters does not lead to unequivocal results. A crucial step is therefore the estimation of the initial parameters for the fitting routine (Maddams 1980). These data were taken from a previous SERR study of cyt^{3+} adsorbed on an Ag electrode (Hildebrandt and Stockburger 1989a). Since these parameters were found to be very similar to those for the states I and II induced on binding of cyt^{3+} to various anionic macromolecular systems (Hildebrandt and Stockburger 1989b) the values can be adopted with some confidence. Consequently, the allowed range for ν_{ij} and $\Delta\nu_{ij}$ was limited to improve the uniqueness of the fit. Since the relative band intensities at a given excitation wavelength are fixed for each cyt^{3+} species, an additional constraint could be introduced into the fitting program. For each mode, *i*, the intensity relative to a reference mode (in the marker band region, ν_3) is defined by the ratio:

$$R_{ij}(\nu_3) = I_{ij}/I_j(\nu_3) \tag{2}$$

The initial values of $R_{ij}(\nu_3)$ can also be adopted from SERR experiments (P. Hildebrandt, unpublished). Finally, it is reasonable to assume that these spectral parameters (R_{ij}, ν_{ij}, and $\Delta\nu_{ij}$) are independent of the relative contributions of the individual species, *j*. Therefore, the data set was enlarged by extending the simulations to the 15 independent RR spectra obtained from the various cyt^{3+}/lipid samples, which differ in the distribution among the three species of cyt^{3+}. It should be mentioned that no experimental conditions were found to measure directly the RR spectra of the pure conformational species.

Based on these considerations, the fitting procedure was carried out according to the following protocol. Initially, the spectral parameters were maintained constant and only the intensities of the three band components were allowed to vary. Then the *R*-factors, frequencies, and half widths were progressively released, but only allowed to vary within 20% for R_{ij} and ± 0.4 cm^{-1} for ν_{ij} and $\Delta\nu_{ij}$. In this way, a first fit was obtained for all measured spectra, yielding an improved set of spectral parameters which were taken as the new initial data for the second fit. This procedure was iterated five times, yielding a final data set which was constant to within $\pm 10\%$ for R_{ij} and ± 0.2 cm^{-1} for ν_{ij} and $\Delta\nu_{ij}$, over all the RR spectra analyzed, and corresponded to the experimental accuracy of measurement. These results are listed in Table 1, and a representative RR spectrum analyzed in this way is shown in Fig. 4C, D. In this connection it is necessary to add that the spectral range simulated included other vibrational modes than ν_4 and ν_3, such as ν_{29} and ν_{20}, whose spectral parameters also depend on the different cyt^{3+} species (P. Hildebrandt, unpublished results). However, the intensities of these modes are too low to provide reliable results for conformational analysis and they were

Table 1. Spectral parameters[a] of the marker bands of cytochrome *c*

System/state	ν_4	$\Delta\nu_4$	ν_3	$\Delta\nu_3$	$R(I_4/I_3)$	$f(\nu_3)$	ν_{10}	$\Delta\nu_{10}$
cyt *c*/H_2O[b]								
cyt^{3+}6cLS	1370.1	15.1	1500.4	11.1	5.55		1633.1	8.8
cyt^{2+}6cLS	1360.4	9.8	1490.5	12.0	13.3			
cyt *c*/lipid								
cyt_I^{3+}6cLS	1369.1	12.2	1499.4	9.6	5.20	6.01	1633.0	8.8
cyt_{II}^{3+}6cLS	1374.0	13.3	1504.6	11.1	5.45	13.66	1637.2	10.8
cyt_{II}^{3+}5cHS	1366.0	13.4	1488.2	15.2	7.50	5.99		
cyt_I^{2+}6cLS	1358.8	9.7	1489.2	10.9	11.0			
cyt_{II}^{2+}6cLS	1361.3	11.1	1491.6	9.2	11.5			
cyt_{II}^{2+}5cHS	1353.1	15.8	1468.4	13.9	4.65			
cyt *c*/electrode[b]								
cyt_I^{3+}6cLS	1369.0	12.0	1499.5	11.4	4.65			
cyt_{II}^{3+}6cLS	1373.6	13.7	1503.1	11.6	6.04			
cyt_{II}^{3+}5cHS	1367.8	11.8	1488.4	12.5	5.90			
cyt_I^{2+}6cLS	1358.8	9.9	1489.8	12.3	13.5			
cyt_{II}^{2+}6cLS	1362.5	13.3	1491.1	12.1	11.5			
cyt_{II}^{2+}5cHS	1354.8	14.4	1467.3	14.4	4.30			

[a] ν_{ij} and $\Delta\nu_{ij}$ are given in cm^{-1}, f_{ij} in M/l
[b] from Hildebrandt and Stockburger (1989a), except for the *R* values (P. Hildebrandt, unpublished results)

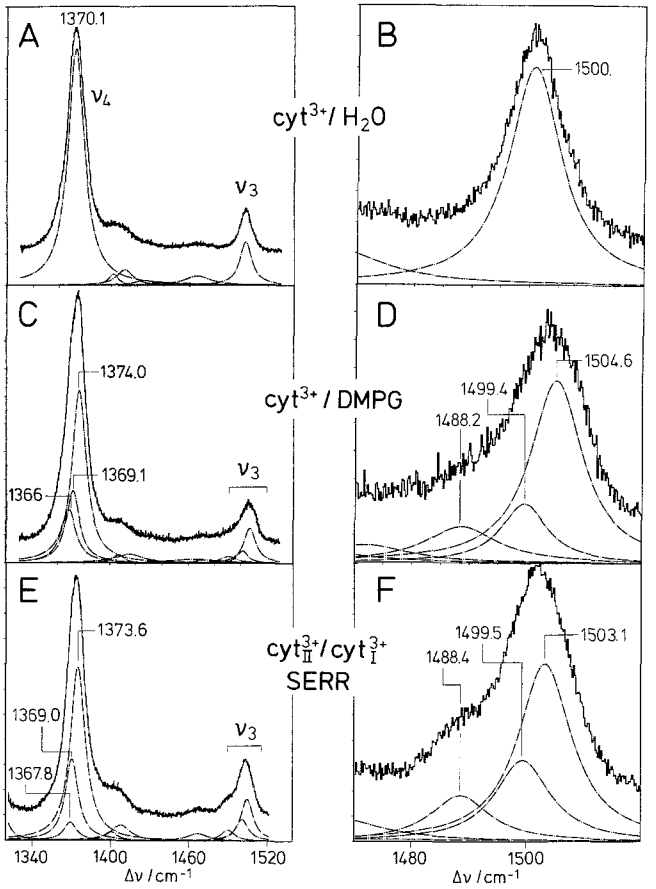

Fig. 4 A–F. High frequency region in the RR spectra of cyt^{3+} excited at 407 nm and recorded at 20 °C. **A** in aqueous solution, **B** bound to DMPG dispersion. **C** SERR spectrum excited at 413 nm of a cyt_I^{3+}/cyt_{II}^{3+} mixture adsorbed on an Ag electrode (cf. Hildebrandt and Stockburger 1989a). Dotted lines are the component Lorentzian profiles, obtained by band fitting as described in the text

therefore simulated by single Lorentzian curves. Finally it is necessary to comment on the reliability of the fitting procedure. Using the same spectral parameters, but quite different initial values for the intensities, the fitting program did not lead to deviations in the calculated intensities of greater than 5%, even for weak components such as the 1488 cm^{-1} band.

Figure 4 E, F gives the SERR spectrum of a mixture of cyt_I^{3+}6cLS, cyt_{II}^{3+}6cLS, and cyt_{II}^{3+}5cHS. The similarity to the RR spectrum of cyt^{3+} bound to DMPG vesicles confirms that these same conformational states are also stabilized on association of cyt^{3+} with lipid membranes.

We like to note that these conformational changes are fully reversible after dissociation of the cyt^{3+}/lipid complexes which can be achieved by increasing the ionic strength. The RR spectra of cyt^{3+}/H_2O and cyt^{3+}/DOPG in the presence of 1.0 *M* KCl were identical.

Finally it should be mentioned that the other spin state marker bands can be analyzed in a similar way (spectra not shown). The spectral parameters so obtained for ν_{10} are listed in Table 1.

Quantitative analysis of the fingerprint region

The band fitting analysis of the low frequency region is more complicated because the precise spectral parameters for the characteristic bands of cyt_I^{3+}6cLS, cyt_{II}^{3+}6cLS, cyt_{II}^{3+}5cHS are not available from the SERR study, thus an alternative approach was chosen to obtain a initial parameter set. Figure 5 shows the RR spectra of the three different cyt^{3+}/lipid complexes in this region. On the left side of the figure (Fig. 5 A, C, E) the ν_3 band region is given for comparison, with the calculated Lorentzian profiles being included to indicate the relative contribu-

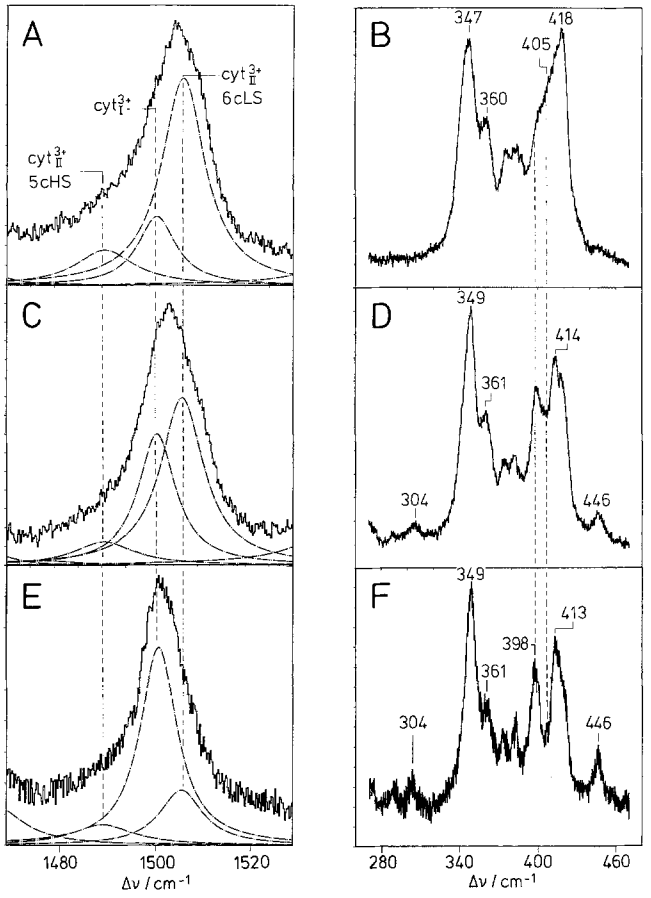

Fig. 5A–F. High frequent (left panel) and low frequency (right panel) regions in the RR spectra of cyt^{3+} bound to different anionic lipid dispersions. **A, B** DMPG recorded at 30 °C, **C, D** DOPG recorded at 22 °C, **E, F** DOPG-DOPC (70 : 30 mole/mole) recorded at 20 °C. Excitation at 407 nm. The dotted lines are the fitted Lorentzian profiles for the high frequency region

tions of the three components. It can readily be seen that the content of cyt^{3+}_{II}6cLS, and to a lesser extent of cyt^{3+}_{II}5cHS, decreases in the order DMPG > DOPG > DOPG-DOPC, with a parallel increase in the cyt^{3+}_{I}6cLS configuration. These trends are reflected by systematic changes in the low frequency spectra (Fig. 5B, D, F) which are given on the right side of the figure. The bands whose intensities decrease with decreasing cyt^{3+}_{I}6cLS content are located at 446, 398, and 305 cm^{-1} and can therefore ascribed to state I.

It is more difficult to identify the bands corresponding to cyt^{3+}_{II}6cLS and cyt^{3+}_{II}5cHS. An increasing RR intensity around 405 cm^{-1} correlates with the increasing contribution of state II. Evidently, a band close to this frequency must arise from the 6cLS configuration, the content of which increases significantly from cyt^{3+}/DOPG-DOPC to cyt^{3+}/DOPG, while that of the 5cHS configuration changes only slightly. From similar arguments, it can be expected that the cyt^{3+}_{II}5cHS configuration exhibits strong bands around 418 and 347 cm^{-1}. However, visual inspection cannot provide reliable spectral parameters for the individual components; it is even not possible to determine the number of bands attributable to each species. These parameters can only be determined from difference spectra corresponding to the pure forms of the cyt^{3+} species.

The difference spectra (denoted Z_j) are obtained by sequential subtractions between the RR spectra corresponding to different compositions (see Fig. 5). They may be represented by linear combinations of the three independent experimental RR spectra B, D, and F, corresponding to Fig. 5B, D, and F:

$$Z_j = k_{jB} \cdot B + k_{jD} \cdot D + k_{jF} \cdot F \qquad (3)$$

where k_{jX} are the weighting factors. Since these constants depend exclusively on the concentration ratios for each species in the three samples, they can be determined from the intensities of the marker bands which were obtained from the fitting program (Fig. 5A, C, E). This subtraction method was extended to 15 independent RR spectra, yielding 5 difference spectra for each species, which were finally combined. The reliability of this procedure depends critically on the normalization of the measured spectra. Although extreme care was taken to maintain the same experimental conditions (concentration, laser power, etc.) for each spectrum, deviations of the normalized intensities of up to 3% for the entire series of measurements cannot be exluded. This can produce a maximal overall error for the calculated weighting factors of ca. 10%. Hence, the spectral parameters which were derived from the difference spectra by band fitting analysis had to be regarded as preliminary and were further refined by iterative analysis of the original spectra following the protocol outlined above. The final set of spectral parameters (Table 2) was used to construct more accurate spectra of the pure components (Fig. 6B, C, D).

Determination of the relative concentrations

Careful inspection of the spectral parameters listed in Table 2 reveals that not all of the bands in the fingerprint region are appropriate for a conformational analysis of cyt^{3+} bound to lipid vesicles RR spectra since some of the bands are too weak or coincide with bands from different species. Nevertheless, including the modes from the marker band region, there are about 7 to 12 bands for each species that are suitable for determination of the relative contributions in samples of unknown composition. Since the spectral parameters of these bands are now well characterized, only three freely adjustable parameters are required for the fitting routine, independent of the total number of bands involved. Once the relative intensities are evaluated in this way, it is necessary to convert them into relative concentrations using (1). The corresponding proportionality factors, f_{ij}, can be adopted from the previous SERR study (Hildebrandt and Stockburger 1989a) assuming that, for a given excitation wavelength, the relative f_{ij} values are the same in the RR and SERR experiments, e.g. adsorption of cyt^{3+} on the Ag electrode, and the accompanying enhancement of the RR scattering, does not affect the Raman cross sections of the individual species in a different way. This assumption appears to be justified since even the relative intensities of the conformational states I and II are independent of the

Table 2. Spectral parameters[a] of the fingerprint bands of ferri-cytochrome *c* in buffer and bound to lipid vesicles

State	Parameter	Band number										
		1	2	3	4	5	6	7	8	9	10	11
cyt^{3+}/H_2O	ν	272.2	289.5	304.8	349.1	361.8	375.0	382.2	398.2	413.3	419.0	446.8
	$\Delta\nu$	11.9	10.2	12.3	9.4	9.7	6.3	7.2	8.5	8.1	7.4	13.8
	R[b]	0.25	0.10	0.21	2.25	0.79	0.33	0.52	1.43	1.00	0.62	0.36
cyt_I^{3+}6cLS/ lipid	ν	270.8	289.7	304.7	348.4	361.7	372.4	381.5	397.9	413.0	420.2	446.2
	$\Delta\nu$	10.7	9.7	12.4	10.0	9.8	7.6	6.9	9.3	8.4	7.9	12.0
	R[b]	0.23	0.11	0.18	1.69	0.47	0.22	0.39	0.99	1.00	0.21	0.25
cyt_{II}^{3+}6cLS/ lipid	ν	–	–	316.5	350.4	362.3	375.4	383.7	–	402.2	419.5	454.6
	$\Delta\nu$	–	–	14.7	11.9	9.5	8.2	9.0	–	10.5	8.4	17.4
	R[b]	–	–	0.09	0.40	0.35	0.20	0.30	–	1.00	0.95	0.08
cyt_{II}^{3+}5sHS/ lipid	ν	–	–	–	343.1	359.9	374.0	387.1	–	408.1	418.5	428.0
	$\Delta\nu$	–	–	–	13.0	11.0	15.3	12.7	–	11.7	12.5	13.1
	R[b]	–	–	–	1.70	0.70	0.43	0.44	–	1.00	0.95	0.09

[a] All ν and $\Delta\nu$ are given in cm^{-1}

[b] The R factors refer to band no. 9; the f_i values for this band are 2.81, 14.42, and 1.0 for cyt_I^{3+}6cLS, cyt_{II}^{3+}6cLS, and cyt_{II}^{3+}5cHS, respectively

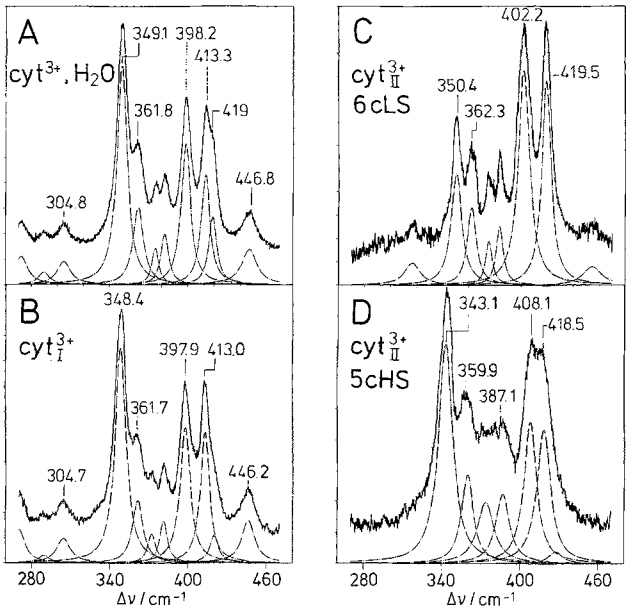

Fig. 6A–D. RR spectra in the low frequency region for the individual species of cyt^{3+} bound to anionic lipid dispersions and dissolved in water. **A** cyt^{3+}/H_2O, **B** cyt_I^{3+}6cLS, **C** cyt_{II}^{3+}6cLS, **D** cyt_{II}^{3+}5cHS. Excitation at 407 nm. The spectra B, C and D are difference spectra obtained by sequential subtraction as described in the text. The dotted lines are the fitted Lorentzian profiles

specific environment in which they are formed (Hildebrandt and Stockburger 1989b). Since the SERR spectra were measured with 413 nm excitation (Hildebrandt and Stockburger 1989a) the corresponding values for 407 nm excitation, which was used in this work, can be obtained by comparing the band intensities of the same sample measured at both excitation wavelengths according to:

$$f_{ij}(407) = f_{ij}(413) \cdot I_{ij}(407)/I_{ij}(413) \quad (4)$$

Conformational changes of the reduced cytochrome c

Figure 7A shows the ν_3 band of ferro-cytochrome *c* in water (cyt^{2+}/H_2O), the frequency of which (1490.5 cm^{-1}) reflects the 6cLS configuration of the reduced heme iron (Partharasathi et al. 1987). In the RR spectrum of cyt^{2+} bound to DMPG (Fig. 7B), a new band emerges at 1468.8 cm^{-1}, indicating a 5cHS configuration. The spectrum of cyt^{2+} bound to lipid is very similar to the SERR spectrum of a mixture of cyt_I^{2+}6cLS, cyt_{II}^{2+}6cLS, and cyt_{II}^{2+}5cHS which is shown in Fig. 7C. This comparison shows that the nature of the conformational changes taking place upon binding to lipid vesicles is the same for both oxidation states of cyt *c*.

Quantitative analysis of the RR spectra of cyt^{2+}/DMPG was performed following the same strategy as for the oxidized cyt *c*. The results of the band fitting are given by the dotted lines in Fig. 7B. In principle, a systematic study can also be carried out for the fingerprint region. However, since the relative intensities of the low frequency bands of cyt_{II}^{2+}6cLS and cyt_{II}^{2+}5cHS are very weak with 407 nm excitation, these spectra are dominated by the RR bands of cyt_I^{2+}6cLS so that a reliable decomposition is not possible for this region.

Structural implications

The formation of state I and state II of cyt^{3+} and cyt^{2+} on binding to anionic lipid vesicles further supports the conclusion that these conformational transitions are induced by the interaction with negatively charged interfaces in general (Hildebrandt and Stockburger 1989b). The close resemblance between the RR spectra of cyt^{3+} (cyt^{2+}) bound to lipid membranes and adsorbed on a metal electrode demonstrates that the structure of these states does not depend critically on the nature of the material from which the surface is composed. Apparently, the electrostatic interactions of the binding domain of

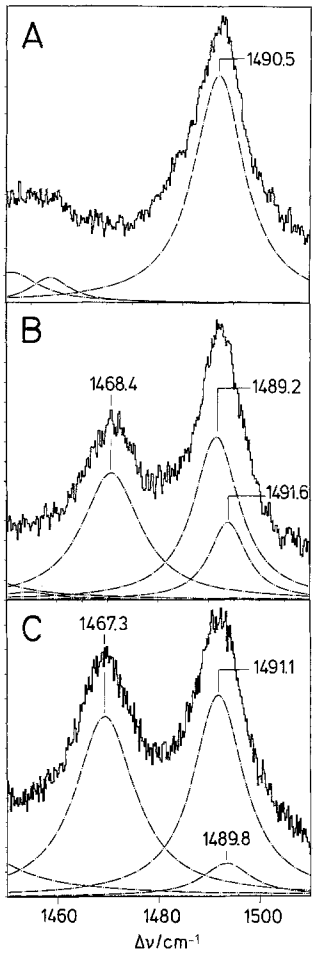

Fig. 7A–C. RR spectra of cyt^{2+} excited at 407 nm and recorded at 20 °C. **A** in aqueous solution, **B** bound to DMPG dispersion. **C** SERR spectrum excited at 413 nm of a cyt_I^{2+}/cyt_{II}^{2+} mixture (cf. Hildebrandt and Stockburger 1989 b). Dotted lines are the fitted Lorentzian profiles

cyt *c* with the electrical double layer of electrodes or biomembranes are comparable. On the other hand, the small differences in frequency between the spectra of state II on the electrode and bound to lipid vesicles may be taken as evidence for different population of conformational substates. This may reflect differences in the details of the electrostatic interactions in the two systems.

Comparison of the RR spectra in both the marker band and the fingerprint band regions shows that the structure of state I is very similar to that of cyt *c* in solution. The small frequency shifts, by about 1 cm^{-1}, of the marker bands (see Table 1) can be attributed to an electrochemical Stark effect at the charged surface. In the fingerprint region, the spectral differences are even smaller (Table 2, Figs. 6A, B). Both cyt^{3+}/H_2O and cyt_I^{3+}6cLS exhibit extremely narrow widths (7 to 10 cm^{-1}) for most modes, indicating that inhomogeneous broadening is small. Since these modes include appreciable contributions from vibrations involving peripheral substituents, this may imply that the heme is rigidly enclosed in the protein matrix, permitting little mobility of the side chains of the heme. Rotations of the substituent groups may have relatively high activation energies, so that specific orientations are preferred, rather than a broad distribution, as is found for porphyrins in solution. Such an interpretation can also account for the large number of bands associated with state I or cyt *c* in solution, possibly reflecting stabilization of individual rotamers.

The transition from state I to state II involves the weakening of the Fe-met bond, establishing a thermal coordination equilibrium. This is accompanied by an opening of the heme crevice (Hildebrandt and Stockburger 1989 a, b). In this way the heme pocket becomes less hydrophobic, as evidenced by the large negative shift of the redox potential for both cyt_{II}6cLS and cyt_{II}5cHS. Hence, one would expect that the steric constraints imposed on the heme by the protein environment in state I are at least partly removed in state II. This is in accord with the low frequency spectra in which the number of bands is reduced and the band half-widths are increased to values between 9 and 12 cm^{-1} for the cyt_{II}^{2+}6cLS (see Fig. 6C and Table 2). Upon dissociation of the sixth ligand, a further loosening of the heme pocket can be inferred from the corresponding values of 10 to 13 cm^{-1} for cyt_{II}^{2+}5cHS (see Fig. 6D and Table 2).

Conclusion

The present study has identified a variety of RR bands which can be used to evaluate the relative populations of the conformational states I and II. The precise determination of the spectral parameters of these bands for each of the three cyt *c* species, cyt_I6cLS, cyt_{II}6cLS, and cyt_{II}5cHS, Tables 1, 2) now allows a full analysis of the RR spectra of cyt *c* bound to lipid vesicles or related systems. Band fitting routines can then be employed which require a minimum of freely adjustable parameters.

The data clearly indicate that the changes in the protein conformation, which take place on binding cyt *c* to negatively charged lipid vesicles, are qualitatively the same as for binding to the silver electrode (Hildebrandt and Stockburger 1989 a). This gives further support to the idea that, docking of cyt *c* onto the negatively charged binding domains of cyt.ox and cyt.red, induces the formation of the conformational states I and II which, in turn, controls the physiological electron transfer reactions (for a detailed model see Hildebrandt and Stockburger 1989 b). Finally, the present findings suggest that both states are stabilized when cyt *c* is bound to the inner mitochondrial membrane so that these conformational equilibria may already be established during the lateral diffusion between the membrane-bound cyt.red and cyt.ox.

Acknowledgements. We thank Dr. M. Stockburger for generous support. Continuous support and encouragement by Prof. A. Weller is greatfully acknowledged.

References

Alshuth T (1985) Kinetische und strukturelle Untersuchungen am Chromophor von Bacteriorhodopsin mit Hilfe zeitaufgelöster Resonanz-Raman-Spektroskopie. P.h.D. Thesis, Universität Göttingen

Azzi A, Fleischer S, Chance B (1969) Cytochrome *c* – phospholipid interactions. Biochem Biophys Res Commun 36:322–327

Brautigan DL, Ferguson-Miller S, Margoliash E (1978) Mitochondrial cytochrome *c*: Preparation and activity of native and chemically modified cytochromes *c*. Methods Enzymol 53D: 128–164

Choi S, Spiro TG (1983) Out-of-plane deformation modes in the resonance Raman spectra of metalloporphyrins and heme proteins. J Am Chem Soc 105:3683–3692

Cotton TM, Schultz SG, Van Duyne RP (1980) Surface enhanced resonance Raman scattering from cytochrome *c* and myoglobin adsorbed on a silver electrode. J Am Chem Soc 102:7960–7962

Devaux PF, Hoatson GL, Favre E, Fellmann P, Farren B, MacKay AL, Bloom M (1986) Interaction of cytochrome *c* with mixed dimyristoylphosphatidylcholine-dimyristoylphosphatidylserine bilayers: a deuterium nuclear magnetic resonance study. Biochemistry 25:3804–3812

Fraser RDB, Suzuki E (1970) Biological applications. In: Blackburn JA (ed) Spectral analysis: methods and techniques. Dekker, New York pp 171–211

de Groot J, Hester RE (1987) Surface enhanced resonance Raman spectroscopy of oxyhemoglobin adsorbed onto colloidal silver. J Phys Chem 91:1693–1696

Heimburg T (1989) Untersuchungen der physikalischen Eigenschaften von biologischen- und Modellmembranen. P.h.D. Thesis, Universität Göttingen

Hildebrandt P, Stockburger M (1989a) Cytochrome *c* at charged interfaces: 1. Conformational and redox equilibria at the electrode/electrolyte interface probed by surface enhanced resonance Raman spectroscopy. Biochemistry 28:6710–6721

Hildebrandt P, Stockburger M (1989b) Cytochrome *c* at charged interfaces: 2. Complexes with negatively charged macromolecular systems studied by resonance Raman spectroscopy. Biochemistry 28:6722–6728

Kimelberg HK, Lee CP, Claude A, Mrena E (1970) Interactions of cytochrome *c* with phospholipid membranes. J Membr Biol 2:235–251

Kitagawa T, Ozaki Y (1987) Infrared and Raman spectra of metalloporphyrins. Struct Bonding 64:71–114

Lee H, Kitagawa T, Abe M, Pandey RK, Leung HK, Smith KM (1986) Characterization of low frequency resonance Raman bands of metalloporphyrin IX. Observation of isotope shifts and normal coordinate treatments. J Mol Struc 146:329–347

Maddams FW (1980) The scope and limitations of curve fitting. Appl Spectrosc 34:245–267

Niki K, Kawasaki Y, Kimura Y, Higuchi Y, Yasuoka N (1989) Surface enhanced Raman scattering of cytochromes c_3 adsorbed on silver electrode and their redox behavior. Langmuir 3:982–986

Parthasarathi N, Hansen C, Yamaguchi S, Spiro TG (1987) Metalloporphorin core size resonance Raman marker bands revisited: Implications for the interpretation of hemoglobin photoproduct Raman frequencies. J Am Chem Soc 109:3865–3871

Peschke J, Möhwald H (1987) Cytochrome *c* interaction with phospholipid monolayers and vesicles. Coll Surf 27:305–326

Rousseau DL (1981) Raman difference spectroscopy as a probe of biological molecules. J Raman Spectrosc 10:94–99

Smulevich G, Spiro TG (1985) Surface enhanced Raman spectroscopic evidence that adsorption on silver particles can denature heme proteins. J Phys Chem 89:5168–5173

Spiro TG (1983) The resonance Raman spectroscopy of metalloporphyrins and heme proteins. In: Lever APB, Gray HB (eds) Iron porphyrins, II. Addison-Wesley, Reading, pp 89–159

Verma AL, Kimura K, Yagi T, Nakamura A, Inokuchi H, Kitagawa T (1989) SERR evidence for enzymatic reduction of cytochrome c_3 adsorbed on Ag colloids. Chem Phys Lett 159:189–192

Wolf CR, Miles JS, Seilman S, Burke MD, Rospendowski BN, Kelly K, Smith WE (1988) Evidence that the catalytic differences of two structurally homologous forms of cytochrome P-450 relate to their heme environments. Biochemistry 27:1597–1603